

Application of the New Mapping Method to Complex Three Coupled Maccari's System Possessing M-Fractional Derivative

Muhammad Bilal Riaz^{*, α ,1}, Aziz Ur Rehman ^{β ,2} and Jan Martinovic ^{γ ,3}

*VSB – Technical University of Ostrava, Ostrava, Czech Republic, ^{α} Department of Computer Science and Mathematics, Lebanese American University, Byblos, Lebanon, ^{β} Department of Mathematics, University of Management and Technology, Lahore, Pakistan.

ABSTRACT In this academic investigation, an innovative mapping approach is applied to complex three coupled Maccari's system to unveil novel soliton solutions. This is achieved through the utilization of M-Truncated fractional derivative with employing the new mapping method and computer algebraic system (CAS) such as Maple. The derived solutions in the form of hyperbolic and trigonometric functions. Our study elucidates a variety of soliton solutions such as periodic, singular, dark, kink, bright, dark-bright solitons solutions. To facilitate comprehension, with certain solutions being visually depicted through 2-dimensional, contour, 3-dimensional, and phase plots depicting bifurcation characteristics utilizing Maple software. Furthermore, the incorporation of M-Truncated derivative enables a more extensive exploration of solution patterns. Our study establishes a connection between computer science and soliton physics, emphasizing the pivotal role of soliton phenomena in advancing simulations and computational modelling. Analytical solutions are subsequently generated through the application of the new mapping method. Following this, a thorough examination of the dynamic nature of the equation is conducted from various perspectives. In essence, understanding the dynamic characteristics of systems is of great importance for predicting outcomes and advancing new technologies. This research significantly contributes to the convergence of theoretical mathematics and applied computer science, emphasizing the crucial role of solitons in scientific disciplines.

KEYWORDS

Complex three coupled Maccari's system
A new mapping method
Soliton patterns
Bifurcation
M-Truncated fractional derivative

INTRODUCTION

In this contemporary era of innovations and development, remarkable advancements have been noted in the field of soliton theory. Soliton phenomena, crucial for augmenting computational capabilities in computer systems, hold particular relevance in applications such as image processing, data analysis and simulations within diverse domains of computer science together with numerous applications in nonlinear optics, engineering, deep water waves, fiber optics, plasma physics, fluid mechanics, mathematical physics, and particularly in scenarios involving the propagation of nonlinear

waves. Soliton models play a crucial role in various applications, including solitary wave-based communication links, fiber-optic, optical pulse compressors, amplifiers, and numerous other mechanisms. Optical solitons play a important role in the realm of telecommunications, serving as a fundamental cornerstone of the industry. Their importance in nonlinear optics is underscored by this distinctive characteristic. Solitons are essentially the outcome of the interplay between non-linearity, which inclines towards increasing the wave slope, and dispersion, which tends to stabilize the wave. Nonlinear physical phenomena is significantly enriched by the presence of precise moving wave solutions in nonlinear partial differential equations (PDEs). Numerous researchers have unveiled a diverse range of solutions across various nonlinear models, including rogue wave solutions, dromion wave solutions, soliton solutions, multi soliton solutions, lumps, and breather solutions. Many efficient techniques have been developed for acquiring precise wave solutions in case of study the

Manuscript received: 5 January 2024,

Revised: 4 April 2024,

Accepted: 4 April 2024.

¹muhammad.bilal.riaz@vsb.cz (Corresponding author)

²prof.azizkhan@gmail.com

³jan.martinovic@vsb.cz

non-linear models, such as, the coupled nonlinear Schrödinger equations (NSEs) and derived the optical soliton solutions by using the Kudryashov R function technique (Das and Saha Ray 2023), for time-fractional perturbed (NSEs) obtained some new soliton solutions with application of the generalized Kudryashov scheme (Das and Saha Ray 2022), for (NSEs) by the application of modified auxiliary technique derived optical solutions and some new optical wave solutions gained by employing the improved $\tan(\phi(\zeta/2))$ -expansion technique to perturbed (NSEs) (Saha Ray and Das 2022), the F-expansion method (A. Filiz and Sonmezoglu 2014; W. B. Rabie and Hamdy 2023), the Jacobi elliptic function expansion method (Zayed and AlurrÖ 2015; Zheng and Feng 2014), and many others have been used in the past.

We employ the new mapping method in our research, a robust approach for addressing nonlinear evolution equations. This method, when applied with specific parameter values, enables the derivation of soliton solutions. New exact soliton solutions derived through this approach align with those obtained through the trial equation method, the first integral method, and the functional variable method. Numerous new results are identified, encompassing in the form of transcendental functions. The versatility of this method is evident through its widespread applications in the literature. For instance, some soliton solutions for two (NSEs) by the application of new mapping method are investigated by Zayed et.al (Zayed and AlurrÖ 2017). Zeng et.al (X. Zeng 2008) developed A new mapping method and discussed its applications to nonlinear partial differential equations. Zayed et.al (E. M. Zayed and Alshehr 2022) investigated Optical wave solutions having Kudryashov's self-phase modulation by using new mapping approach.

The versatile and valuable impacts of fractional calculus in the field of electrical engineering, electrochemistry, control theory, electromagnetism, mechanics, image processing, bioengineering, physics, finance, fluid dynamics, and many others make it a valuable tool for study. Fractional derivatives not only keep the record of the present but also the past, so they are very suitable and accurate when the system has long-term memory. It has several applications in physical science as well as in other areas such as biology, astrophysics, ecology, geology and chemistry. The mechanism of non-Newtonian models is elaborated successfully with the fractional calculus in the past decades due to its simple and elegant description of the complexity of its behaviour. One of the important feature and most commonly known name of non-Newtonian fluid is viscoelastic fluid that which exhibit the behaviour of elasticity and viscosity. Such types of fluid models have great implications in various fields namely polymerization, industrial as well as mechanical engineering and also in the field of auto mobile industry due to its significance.

Fractional calculus is very helpful in the interpretation of the viscoelastic nature of the materials. Taking into account the enormous mentioned properties, many researchers paid attention to analyse the fractional behaviour of different models directly or indirectly in case of derivatives when it is considered as non-integer order from. Fractional calculus, emerging from the traditional calculus such as derivative and integral operators, much like fractional exponents evolving from integer values, constitutes a distinct field of mathematical study. Certainly. Real-world processes, by and large, exhibit characteristics of fractional-order systems. The effectiveness of Fractional Calculus (FC) applications can be attributed to the high accuracy of these innovative fractional-order models as compared to traditional models. The fractional order model introduces greater degrees of freedom than the corresponding

classical model, contributing to its superior performance. A differential equation containing fractional integrals, derivatives or both is described as a Fractional Equation (FE).

Recognition of the importance of such equations has steadily increased over the past decade. Diverse applications have surfaced, including wave propagation in porous media or complex (Zaslavsky 2002), fractional order modified Duffing systems (Ge and Ou 2008), Ginzburg–Landau model (Zhu and Gao 2023), regularized symmetric long wave equation flow models in deep water (Senol 2020), in physical and engineering sciences fractional Boussinesq type equations (Ellahi and Khan 2018), and Korteweg–de Vries equations taking coefficients variable (Wang and Li 2018). The spectrum of fractional derivative operators encompasses various types, such as Beta-fractional derivative (Rafiq and Kamran 2022), Atangana–Baleanu–Riemann fractional derivative (Khater and Kumar 2020), Caputo–Fabrizio derivative (Naeem and Zaland 2022), and truncated M-fractional derivatives (Mohammed and Abouelregal 2023; Alabedalhadi and Alhazmi 2023).

The aim of this paper is to clarify how the soliton solutions of the complex three coupled Maccari's system are influenced by the M-fractional derivative operator, by using the New Mapping Method. The importance of the M-fractional derivative lies in its capacity to incorporate the features of both fractional and integer order derivatives. This serves as a generalization of numerous fractional derivatives, preserving essential characteristics of integer-order derivatives. Our findings reveal that employing straightforward schemes and solvable ordinary differential equations (ODEs) facilitates the easy derivation of various exact-wave solutions for complex NLFPEs.

Notably, the solution of this ODE has been achieved using the New mapping method technique, the obtained results are novel compared to existing literature to examine soliton patterns. Following this, we have explored the dynamics of the analyzed equation by employing bifurcation theory. As a result, phase portraits illustrates the bifurcation features of the model under various initial conditions has been conducted. A bifurcation theory refers to a qualitative transformation to unveil the dynamical system characteristics, provides the modification of involving parameters. The primary objective of this study is to unveil novel exact soliton solutions for the considered system with employing the new mapping method and analyzed the behaviour of differential equations (DEs) through the bifurcation analysis.

This manuscript is structured as follows: Described the basic definition and properties of M-fractional derivative in Section 2. Section 3 presented the fractional model being studied. Section 4 provides an overview of the renowned new mapping method. In Section 5, wave solutions discovered by employing this method along with several figures displayed. Section 6 involves the illustration of bifurcation analysis and discussed the behaviour of fixed points through phase portraits. Finally, Section 7 presents the comprehensive summary of the obtained results from the study.

FUNDAMENTAL CONCEPTS OF FRACTIONAL CALCULUS

In this part, some basic concepts of the fractional operator used in this article are given.

Truncated-M Fractional Derivative

Definition 1 The truncated one parameter Mittag-Leffler function is given below (Vanterler 2018):

$${}_i E_{\omega}(G) = \sum_{j=0}^i \frac{G^j}{\Gamma(\omega j + 1)},$$

where $\omega > 0$ and $G \in \mathbb{C}$.

Definition 2 Let $R : [0, \infty) \rightarrow \mathbb{R}$ and $\delta \in (0, 1)$. The truncated M -derivative of function R of order ϑ is defined by:

$$\mathcal{D}_M^{\vartheta, \omega} R(t) = \lim_{\varepsilon \rightarrow 0} \frac{R(t + {}_i E_\omega(\varepsilon t^{-\vartheta})) - R(t)}{\varepsilon},$$

for $t > 0$ and ${}_i E_\omega(\cdot)$, where $\omega > 0$.

Theorem 1 Suppose that R is a differentiable function of order ϑ at $t_0 > 0$, where $\vartheta \in (0, 1]$ and $\omega > 0$. Then, R is continuous at t_0 .

Theorem 2 Assuming $\vartheta \in (0, 1]$, $\omega > 0$, $\alpha, \beta \in \mathbb{R}$, and R, S are ϑ -differentiable at $t > 0$, then:

- 1- ${}_i \mathcal{D}_M^{\vartheta, \omega} (\alpha R(t) + \beta S(t)) = \alpha {}_i \mathcal{D}_M^{\vartheta, \omega} (R(t)) + \beta {}_i \mathcal{D}_M^{\vartheta, \omega} (S(t))$.
- 2- ${}_i \mathcal{D}_M^{\vartheta, \omega} (R(t) \cdot S(t)) = R(t) {}_i \mathcal{D}_M^{\vartheta, \omega} (S(t)) + S(t) {}_i \mathcal{D}_M^{\vartheta, \omega} (R(t))$.
- 3- ${}_i \mathcal{D}_M^{\vartheta, \omega} \left(\frac{R(t)}{S(t)} \right) = \frac{R(t) {}_i \mathcal{D}_M^{\vartheta, \omega} (S(t)) - S(t) {}_i \mathcal{D}_M^{\vartheta, \omega} (R(t))}{[S(t)]^2}$.
- 4- ${}_i \mathcal{D}_M^{\vartheta, \omega} (\delta) = 0$, where δ is a constant.
- 5- If $R(t)$ is differentiable, then ${}_i \mathcal{D}_M^{\vartheta, \omega} (R)(t) = \frac{t^{1-\vartheta}}{\Gamma(\vartheta+1)} \frac{dR(t)}{dt}$.

FRACTIONAL GOVERNING MODEL WITH MATHEMATICAL ANALYSIS

The M -fractional three-coupled nonlinear Maccari's system, as depicted in (Emad and Lanre 2021), elucidates the propagation of isolated waves within a limited spatial domain. This phenomenon is relevant to various fields such as hydrodynamics, optical communications and plasma physics.

$$\begin{cases} iD_{M,t}^{x,\gamma} \Psi + \Psi_{xx} + \Pi \Psi = 0, \\ iD_{M,t}^{x,\gamma} \Phi + \Phi_{xx} + \Pi \Phi = 0, \\ iD_{M,t}^{x,\gamma} \Omega + \Omega_{xx} + \Pi \Omega = 0, \\ iD_{M,t}^{x,\gamma} \Pi + \Pi_y + (|\Psi + \Phi + \Omega|^2)_x = 0. \end{cases} \quad (1)$$

Let us consider the following transformations:

$$\begin{cases} \Psi(x, y, t) = \Psi(\zeta) \times \exp\left(\iota \left(\kappa_1 x + \nu y + \theta \frac{\Gamma(\gamma+1)}{\alpha} t^\alpha\right) + \kappa\right), \\ \Phi(x, y, t) = \Phi(\zeta) \times \exp\left(\iota \left(\kappa_1 x + \nu y + \theta \frac{\Gamma(\gamma+1)}{\alpha} t^\alpha\right) + \kappa\right), \\ \Omega(x, y, t) = \Omega(\zeta) \times \exp\left(\iota \left(\kappa_1 x + \nu y + \theta \frac{\Gamma(\gamma+1)}{\alpha} t^\alpha\right) + \kappa\right), \\ \Pi(x, y, t) = \Pi(\zeta) \quad \text{where} \quad \zeta = \lambda \left(x + y - 2\beta \frac{\Gamma(\gamma+1)}{\alpha} t^\alpha\right). \end{cases} \quad (2)$$

In this context, the variables κ_1, θ, ν , and β represent the unknowns, with κ serving as the arbitrary constant. Upon substituting Equation (2) into Equation (1), both the real and imaginary components are derived such as, Real parts:

$$\begin{cases} \lambda^2 \Psi'' - (\theta + \kappa_1^2) \Psi + \Psi \Pi = 0, \\ \lambda^2 \Phi'' - (\theta + \kappa_1^2) \Phi + \Phi \Pi = 0, \\ \lambda^2 \Omega'' - (\theta + \kappa_1^2) \Omega + \Omega \Pi = 0, \\ \lambda(1 - 2\beta) \Pi' + \lambda ((\Psi + \Phi + \Omega)^2)' = 0. \end{cases} \quad (3)$$

and its imaginary parts:

$$(-2\beta + 2\kappa_1) \Psi' = 0, (-2\beta + 2\kappa_1) \Phi' = 0, (-2\beta + 2\kappa_1) \Omega' = 0. \quad (4)$$

By Equation Eq.(4), imply $\beta = \kappa_1$. Integrating the fourth equation of system (3) yields

$$\Pi = -\frac{(\Psi + \Phi + \Omega)^2}{1 - 2\kappa_1} \quad (5)$$

Replacing (5) in the system (3), yields

$$\begin{cases} \lambda^2 \Psi'' - (\theta + \kappa_1^2) \Psi - \frac{(\Psi + \Phi + \Omega)^2}{1 - 2\kappa_1} \Psi = 0, \\ \lambda^2 \Phi'' - (\theta + \kappa_1^2) \Phi - \frac{(\Psi + \Phi + \Omega)^2}{1 - 2\kappa_1} \Phi = 0, \\ \lambda^2 \Omega'' - (\theta + \kappa_1^2) \Omega - \frac{(\Psi + \Phi + \Omega)^2}{1 - 2\kappa_1} \Omega = 0. \end{cases} \quad (6)$$

Taking $\Phi = \kappa_2 \Psi$ and $\Omega = c\Psi$ in the system (6), we obtain

$$\lambda^2 \Psi'' - (\theta + \kappa_1^2) \Psi - \frac{(1 + \kappa_2 + c)^2}{1 - 2\kappa_1} \Psi^3 = 0 \quad (7)$$

OVERVIEW OF THE RECENTLY INTRODUCED NEW MAPPING METHOD

Consider the non-linear PDE :

$$P(\Psi, \Psi_x, \Psi_t, \Psi_{xx}, \Psi_t, \dots) = 0 \quad (8)$$

In this context, where P is a polynomial in Ψ involving its partial derivatives, specifically the highest order derivatives and nonlinear terms and Ψ is a function of x and t , i.e, $\Psi = \Psi(x, t)$ which is an unknown function. The fundamental procedures of the widely recognized new mapping method (X. Zeng 2008) can be outlined as follows:

Step 1. The transformation of travelling wave

$$\Psi(x, t) = \Psi(\zeta), \quad \zeta = x - ct \quad (9)$$

where c represent a constant, after applying the transformation, Eq. (8) reduces into to the following non-linear (ODE):

$$G(\Psi, \Psi', \Psi'', \dots) = 0 \quad (10)$$

Here, G represents a polynomial involving $\Psi(\zeta)$ and its derivatives with respect to ζ .

Step 2. We assume that the solution to Equation (10) written in the following form:

$$\Psi(\zeta) = \sum_{i=0}^{2N} \alpha_i F^i(\zeta) \quad (11)$$

Here, $F(\zeta)$ fulfills a first-order nonlinear ordinary differential equation:

$$(F')^2(\zeta) = pF^2(\zeta) + \frac{1}{2}qF^4(\zeta) + \frac{1}{3}sF^6(\zeta) + r \quad (12)$$

In this context, constants α_i (where i ranges from 0 to $2N$), along with the constants p, q, s , and r , are to be determined, but both s and α_{2N} must be non-zero.

Step 3. We ascertain the balancing number N for Equation (11) by equating the highest-order derivatives with the highest nonlinear terms in Equation (10).

Step 4. By substituting Eq.(11) together with Eq. (12) into Eq. (10) and aggregating all the coefficients of $F^m (F')^n$ (where $m = 0, 1, 2, \dots$) and $(n = 0, 1)$, subsequent setting of these coefficients to zero leads to a system of algebraic equations. These equations can be effectively solved using Maple software to determine the values of unknowns such as, α_i (where $i = 0, 1, 2, \dots, 2N$), p, q, s, r , and c .

Step 5. It is widely acknowledged (Zayed and AlurrÖ 2017; X. Zeng 2008; E. M. Zayed and Alshehr 2022) that Eq. (12) possesses sets of solutions, outlined as follows:

$$F_1(\zeta) = 4 \left(-\frac{p \tanh^2 \left(\epsilon \sqrt{-\frac{p}{3}} \zeta \right)}{3q \left(3 + \tanh^2 \left(\epsilon \sqrt{-\frac{p}{3}} \zeta \right) \right)} \right)^{\frac{1}{2}},$$

$$p < 0, q > 0, s = \frac{3q^2}{16p}, r = \frac{16p^2}{27q},$$

$$F_2(\zeta) = 4 \left(-\frac{p \coth^2 \left(\epsilon \sqrt{-\frac{p}{3}} \zeta \right)}{3q \left(3 + \coth^2 \left(\epsilon \sqrt{-\frac{p}{3}} \zeta \right) \right)} \right)^{\frac{1}{2}},$$

$$p < 0, q > 0, s = \frac{3q^2}{16p}, r = \frac{16p^2}{27q},$$

$$F_3(\zeta) = 4 \left(\frac{p \tan^2 \left(\epsilon \sqrt{\frac{p}{3}} \zeta \right)}{3q \left(3 - \tan^2 \left(\epsilon \sqrt{\frac{p}{3}} \zeta \right) \right)} \right)^{\frac{1}{2}},$$

$$p > 0, q < 0, s = \frac{3q^2}{16p}, r = \frac{16p^2}{27q},$$

$$F_4(\zeta) = 4 \left(\frac{p \cot^2 \left(\epsilon \sqrt{\frac{p}{3}} \zeta \right)}{3q \left(3 - \cot^2 \left(\epsilon \sqrt{\frac{p}{3}} \zeta \right) \right)} \right)^{\frac{1}{2}},$$

$$p > 0, q < 0, s = \frac{3q^2}{16p}, r = \frac{16p^2}{27q},$$

$$F_5(\zeta) = \left(-\frac{2p}{q} (1 + \tanh(\epsilon \sqrt{p} \zeta)) \right)^{\frac{1}{2}}, p > 0, s = \frac{3q^2}{16p}, r = 0,$$

$$F_6(\zeta) = \left(-\frac{2p}{q} (1 + \coth(\epsilon \sqrt{p} \zeta)) \right)^{\frac{1}{2}}, p > 0, s = \frac{3q^2}{16p}, r = 0,$$

$$F_7(\zeta) = \left(-\frac{6pq \operatorname{sech}^2(\sqrt{p} \zeta)}{3q^2 - 4ps(1 + \epsilon \tanh(\sqrt{p} \zeta))^2} \right)^{\frac{1}{2}}, p > 0, r = 0,$$

$$F_8(\zeta) = \left(\frac{6pq \operatorname{csch}^2(\sqrt{p} \zeta)}{3q^2 - 4ps(1 + \epsilon \coth(\sqrt{p} \zeta))^2} \right)^{\frac{1}{2}}, p > 0, r = 0,$$

$$F_9(\zeta) = \left(-\frac{6p \operatorname{sech}^2(\sqrt{p} \zeta)}{3q + 4\epsilon \sqrt{3ps} \tanh(\sqrt{p} \zeta)} \right)^{\frac{1}{2}}, p > 0, s > 0, r = 0,$$

$$F_{10}(\zeta) = \left(\frac{6p \operatorname{csch}^2(\sqrt{p} \zeta)}{3q + 4\epsilon \sqrt{3ps} \coth(\sqrt{p} \zeta)} \right)^{\frac{1}{2}}, p > 0, s > 0, r = 0,$$

$$F_{11}(\zeta) = \left(-\frac{6p \operatorname{sec}^2(\sqrt{-p} \zeta)}{3q + 4\epsilon \sqrt{-3ps} \tan(\sqrt{-p} \zeta)} \right)^{\frac{1}{2}}, p < 0, s > 0, r = 0,$$

$$F_{12}(\zeta) = \left(-\frac{6p \operatorname{csc}^2(\sqrt{-p} \zeta)}{3q + 4\epsilon \sqrt{-3ps} \cot(\sqrt{-p} \zeta)} \right)^{\frac{1}{2}}, p < 0, s > 0, r = 0$$

$$F_{13}(\zeta) = 2 \left(\frac{3p \operatorname{sech}^2(\epsilon \sqrt{p} \zeta)}{2\sqrt{M} - (\sqrt{M} + 3q) \operatorname{sech}^2(\epsilon \sqrt{p} \zeta)} \right)^{\frac{1}{2}},$$

$$p > 0, q < 0, s < 0, M > 0, r = 0 \quad (13)$$

$$F_{14}(\zeta) = 2 \left(\frac{3p \operatorname{csch}^2(\epsilon \sqrt{p} \zeta)}{2\sqrt{M} + (\sqrt{M} - 3q) \operatorname{csch}^2(\epsilon \sqrt{p} \zeta)} \right)^{\frac{1}{2}},$$

$$p > 0, q < 0, s < 0, M > 0, r = 0,$$

$$F_{15}(\zeta) = 2 \left(\frac{-3p \operatorname{sec}^2(\epsilon \sqrt{-p} \zeta)}{2\sqrt{M} - (\sqrt{M} - 3q) \operatorname{sec}^2(\epsilon \sqrt{-p} \zeta)} \right)^{\frac{1}{2}},$$

$$p < 0, q > 0, s < 0, M > 0, r = 0,$$

$$F_{16}(\zeta) = 2 \left(\frac{3p \operatorname{csc}^2(\epsilon \sqrt{-p} \zeta)}{2\sqrt{M} - (\sqrt{M} + 3q) \operatorname{csc}^2(\epsilon \sqrt{-p} \zeta)} \right)^{\frac{1}{2}},$$

$$p < 0, q > 0, s < 0, M > 0, r = 0,$$

$$F_{17}(\zeta) = 2 \left(\frac{3p}{\epsilon \sqrt{M} \cosh(2\sqrt{p} \zeta) - 3q} \right)^{\frac{1}{2}}, p > 0, M > 0, r = 0,$$

$$F_{18}(\zeta) = 2 \left(\frac{3p}{\epsilon \sqrt{M} \cos(2\sqrt{-p} \zeta) - 3q} \right)^{\frac{1}{2}}, p < 0, M > 0, r = 0,$$

$$F_{19}(\zeta) = 2 \left(\frac{3p}{\epsilon \sqrt{M} \sin(2\sqrt{-p} \zeta) - 3q} \right)^{\frac{1}{2}}, p < 0, M > 0, r = 0$$

$$F_{20}(\zeta) = 2 \left(\frac{3p}{\epsilon \sqrt{-M} \sinh(2\sqrt{p} \zeta) - 3q} \right)^{\frac{1}{2}}, p > 0, M < 0, r = 0,$$

where $M = 9q^2 - 48ps$ and $\epsilon = \pm 1$.

Step 6. By substituting the values of α_i , p , q , s , r , and c , along with the solutions of Eq. (12) provided in Step 5, into Eq. (11), we obtain the precise solutions for Eq. (8).

EXPLICIT SOLUTIONS OF THE EQUATION

In this section the primary objective to obtain the precise solutions for the model under examination. Calculating the value of N involves the application of the homogeneous balancing principle to Eq. (7). By setting Ψ'' and Ψ^3 in Eq. (7) equal to each other, yielding $3N = N + 2$, we deduce that $N = 1$. Consequently, for $N = 1$, the solution of the system can be expressed as follows:

$$\Psi(\zeta) = \Lambda_0 + \Lambda_1 F(\zeta) + \Lambda_2 F^2(\zeta). \quad (14)$$

By substituting Eq. (14) into Eq. (7) along with Eq. (12), a system of equations is formed by equating the coefficients of various powers of $F(\zeta)$ to zero. The utilization of Maple software in solving this system yields the following efficacious solution:

$$p = -\left(\frac{A+3B\kappa^2}{4} \right), \quad q = \mp \frac{2\kappa\sqrt{-6Bs}}{3}, \quad (15)$$

$$\Lambda_0 = \Theta, \Lambda_1 = 0, \quad \Lambda_2 = \pm \frac{2\sqrt{-6Bs}}{3B}$$

where,

$$\Theta = \frac{\left(\left(3\sqrt{3} \sqrt{\frac{A^3 - 72sr^2}{B}} B + 18\sqrt{-6Bs} r \right) B \right)^{\frac{3}{2}} - 3AB}{3B \left(\left(3\sqrt{3} \sqrt{\frac{A^3 - 72sr^2}{B}} B + 18\sqrt{-6Bs} r \right) B \right)^{\frac{1}{2}}},$$

$$A = -\frac{(\theta + \kappa_1^2)}{\lambda^2}, \quad B = -\frac{(1 + \kappa_2 + c)^2}{\lambda^2(1 - 2\kappa_1)}.$$

By plugging above values in Eq.(14) which becomes $\Psi(\zeta) = \Theta \pm \frac{2\sqrt{-6Bs}}{3B} F^2(\zeta)$ and employing the transformation mentioned in Eq.(12), the solutions of system (1) are as follows,

• **Type 1:** For $p < 0, q > 0, s = \frac{3q^2}{16p}$ and $r = \frac{16p^2}{27q}$, we have

$$\begin{cases} \Psi_1(x, y, t) = \left[\Theta \pm \frac{32\sqrt{-6Bs}}{3B} \left(-\frac{p \tanh^2(\epsilon\sqrt{-\frac{p}{3}\zeta})}{3q(3 + \tanh^2(\epsilon\sqrt{-\frac{p}{3}\zeta}))} \right) \right] \\ \quad \times \left(\exp \left(\iota \left(\kappa_1 x + \nu y + \theta \frac{\Gamma(\gamma+1)}{\alpha} t^\alpha \right) \right) + \kappa \right), \\ \Phi_1(x, y, t) = \kappa_2 \left[\Theta \pm \frac{32\sqrt{-6Bs}}{3B} \left(-\frac{p \tanh^2(\epsilon\sqrt{-\frac{p}{3}\zeta})}{3q(3 + \tanh^2(\epsilon\sqrt{-\frac{p}{3}\zeta}))} \right) \right] \\ \quad \times \left(\exp \left(\iota \left(\kappa_1 x + \nu y + \theta \frac{\Gamma(\gamma+1)}{\alpha} t^\alpha \right) \right) + \kappa \right), \\ \Omega_1(x, y, t) = c \left[\Theta \pm \frac{32\sqrt{-6Bs}}{3B} \left(-\frac{p \tanh^2(\epsilon\sqrt{-\frac{p}{3}\zeta})}{3q(3 + \tanh^2(\epsilon\sqrt{-\frac{p}{3}\zeta}))} \right) \right] \\ \quad \times \left(\exp \left(\iota \left(\kappa_1 x + \nu y + \theta \frac{\Gamma(\gamma+1)}{\alpha} t^\alpha \right) \right) + \kappa \right), \end{cases} \quad (16)$$

• **Type 2:** For $p < 0, q > 0, s = \frac{3q^2}{16p}$ and $r = \frac{16p^2}{27q}$, we have

$$\begin{cases} \Psi_1(x, y, t) = \left[\Theta \pm \frac{32\sqrt{-6Bs}}{3B} \left(-\frac{p \operatorname{coth}^2(\epsilon\sqrt{-\frac{p}{3}\zeta})}{3q(3 + \operatorname{coth}^2(\epsilon\sqrt{-\frac{p}{3}\zeta}))} \right) \right] \\ \quad \times \left(\exp \left(\iota \left(\kappa_1 x + \nu y + \theta \frac{\Gamma(\gamma+1)}{\alpha} t^\alpha \right) \right) + \kappa \right), \\ \Phi_1(x, y, t) = \kappa_2 \left[\Theta \pm \frac{32\sqrt{-6Bs}}{3B} \left(-\frac{p \operatorname{coth}^2(\epsilon\sqrt{-\frac{p}{3}\zeta})}{3q(3 + \operatorname{coth}^2(\epsilon\sqrt{-\frac{p}{3}\zeta}))} \right) \right] \\ \quad \times \left(\exp \left(\iota \left(\kappa_1 x + \nu y + \theta \frac{\Gamma(\gamma+1)}{\alpha} t^\alpha \right) \right) + \kappa \right), \\ \Omega_1(x, y, t) = c \left[\Theta \pm \frac{32\sqrt{-6Bs}}{3B} \left(-\frac{p \operatorname{coth}^2(\epsilon\sqrt{-\frac{p}{3}\zeta})}{3q(3 + \operatorname{coth}^2(\epsilon\sqrt{-\frac{p}{3}\zeta}))} \right) \right] \\ \quad \times \left(\exp \left(\iota \left(\kappa_1 x + \nu y + \theta \frac{\Gamma(\gamma+1)}{\alpha} t^\alpha \right) \right) + \kappa \right), \end{cases} \quad (17)$$

• **Type 3:** For $p > 0, q < 0, s = \frac{3q^2}{16p}$ and $r = \frac{16p^2}{27q}$, we have

$$\begin{cases} \Psi_1(x, y, t) = \left[\Theta \pm \frac{32\sqrt{-6Bs}}{3B} \left(\frac{p \tan^2(\epsilon\sqrt{\frac{p}{3}\zeta})}{3q(3 - \tan^2(\epsilon\sqrt{\frac{p}{3}\zeta}))} \right) \right] \\ \quad \times \left(\exp \left(\iota \left(\kappa_1 x + \nu y + \theta \frac{\Gamma(\gamma+1)}{\alpha} t^\alpha \right) \right) + \kappa \right), \\ \Phi_1(x, y, t) = \kappa_2 \left[\Theta \pm \frac{32\sqrt{-6Bs}}{3B} \left(\frac{p \tan^2(\epsilon\sqrt{\frac{p}{3}\zeta})}{3q(3 - \tan^2(\epsilon\sqrt{\frac{p}{3}\zeta}))} \right) \right] \\ \quad \times \left(\exp \left(\iota \left(\kappa_1 x + \nu y + \theta \frac{\Gamma(\gamma+1)}{\alpha} t^\alpha \right) \right) + \kappa \right), \\ \Omega_1(x, y, t) = c \left[\Theta \pm \frac{32\sqrt{-6Bs}}{3B} \left(\frac{p \tan^2(\epsilon\sqrt{\frac{p}{3}\zeta})}{3q(3 - \tan^2(\epsilon\sqrt{\frac{p}{3}\zeta}))} \right) \right] \\ \quad \times \left(\exp \left(\iota \left(\kappa_1 x + \nu y + \theta \frac{\Gamma(\gamma+1)}{\alpha} t^\alpha \right) \right) + \kappa \right), \end{cases} \quad (18)$$

• **Type 4:** For $p > 0, q < 0, s = \frac{3q^2}{16p}$ and $r = \frac{16p^2}{27q}$, we have

$$\begin{cases} \Psi_4(x, y, t) = \left[\Theta \pm \frac{32\sqrt{-6Bs}}{3B} \left(\frac{p \cot^2(\epsilon\sqrt{\frac{p}{3}\zeta})}{3q(3 - \cot^2(\epsilon\sqrt{\frac{p}{3}\zeta}))} \right) \right] \\ \quad \times \left(\exp \left(\iota \left(\kappa_1 x + \nu y + \theta \frac{\Gamma(\gamma+1)}{\alpha} t^\alpha \right) \right) + \kappa \right), \\ \Phi_4(x, y, t) = \kappa_2 \left[\Theta \pm \frac{32\sqrt{-6Bs}}{3B} \left(\frac{p \cot^2(\epsilon\sqrt{\frac{p}{3}\zeta})}{3q(3 - \cot^2(\epsilon\sqrt{\frac{p}{3}\zeta}))} \right) \right] \\ \quad \times \left(\exp \left(\iota \left(\kappa_1 x + \nu y + \theta \frac{\Gamma(\gamma+1)}{\alpha} t^\alpha \right) \right) + \kappa \right), \\ \Omega_4(x, y, t) = c \left[\Theta \pm \frac{32\sqrt{-6Bs}}{3B} \left(\frac{p \cot^2(\epsilon\sqrt{\frac{p}{3}\zeta})}{3q(3 - \cot^2(\epsilon\sqrt{\frac{p}{3}\zeta}))} \right) \right] \\ \quad \times \left(\exp \left(\iota \left(\kappa_1 x + \nu y + \theta \frac{\Gamma(\gamma+1)}{\alpha} t^\alpha \right) \right) + \kappa \right), \end{cases} \quad (19)$$

• **Type 5:** For $p > 0, s = \frac{3q^2}{16p}$ and $r = 0$, we have

$$\begin{cases} \Psi_5(x, y, t) = \left[\Theta \pm \frac{2\sqrt{-6Bs}}{3B} \left(-\frac{2p}{q} (1 + \tanh(\epsilon\sqrt{p}\zeta)) \right) \right] \\ \quad \times \left(\exp \left(\iota \left(\kappa_1 x + \nu y + \theta \frac{\Gamma(\gamma+1)}{\alpha} t^\alpha \right) \right) + \kappa \right), \\ \Phi_5(x, y, t) = \kappa_2 \left[\Theta \pm \frac{2\sqrt{-6Bs}}{3B} \left(-\frac{2p}{q} (1 + \tanh(\epsilon\sqrt{p}\zeta)) \right) \right] \\ \quad \times \left(\exp \left(\iota \left(\kappa_1 x + \nu y + \theta \frac{\Gamma(\gamma+1)}{\alpha} t^\alpha \right) \right) + \kappa \right), \\ \Omega_5(x, y, t) = c \left[\Theta \pm \frac{2\sqrt{-6Bs}}{3B} \left(-\frac{2p}{q} (1 + \tanh(\epsilon\sqrt{p}\zeta)) \right) \right] \\ \quad \times \left(\exp \left(\iota \left(\kappa_1 x + \nu y + \theta \frac{\Gamma(\gamma+1)}{\alpha} t^\alpha \right) \right) + \kappa \right), \end{cases} \quad (20)$$

• **Type 6:** For $p > 0, s = \frac{3q^2}{16p}$ and $r = 0$, we have

$$\begin{cases} \Psi_6(x, y, t) = \left[\Theta \pm \frac{2\sqrt{-6Bs}}{3B} \left(-\frac{2p}{q} (1 + \operatorname{coth}(\epsilon\sqrt{p}\zeta)) \right) \right] \\ \quad \times \left(\exp \left(\iota \left(\kappa_1 x + \nu y + \theta \frac{\Gamma(\gamma+1)}{\alpha} t^\alpha \right) \right) + \kappa \right), \\ \Phi_6(x, y, t) = \kappa_2 \left[\Theta \pm \frac{2\sqrt{-6Bs}}{3B} \left(-\frac{2p}{q} (1 + \operatorname{coth}(\epsilon\sqrt{p}\zeta)) \right) \right] \\ \quad \times \left(\exp \left(\iota \left(\kappa_1 x + \nu y + \theta \frac{\Gamma(\gamma+1)}{\alpha} t^\alpha \right) \right) + \kappa \right), \\ \Omega_6(x, y, t) = c \left[\Theta \pm \frac{2\sqrt{-6Bs}}{3B} \left(-\frac{2p}{q} (1 + \operatorname{coth}(\epsilon\sqrt{p}\zeta)) \right) \right] \\ \quad \times \left(\exp \left(\iota \left(\kappa_1 x + \nu y + \theta \frac{\Gamma(\gamma+1)}{\alpha} t^\alpha \right) \right) + \kappa \right), \end{cases} \quad (21)$$

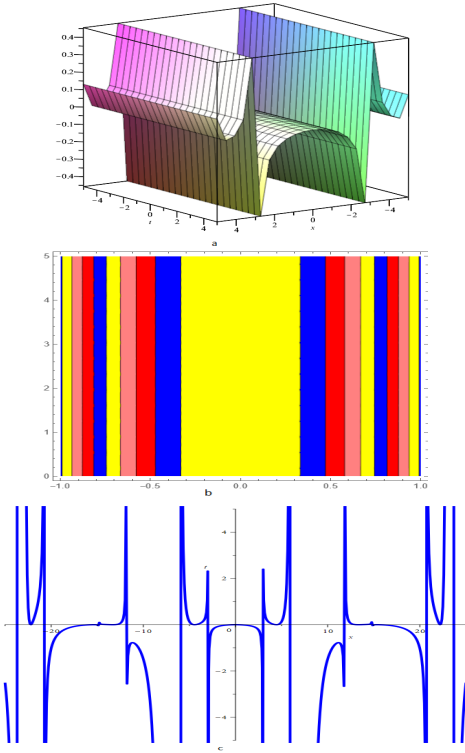


Figure 1 Figures (a),(b) and (c) represents 3D, Contour and 2D plots respectively for $\Psi_3(x, y, t)$ corresponding to the values $\kappa = 0.5, \epsilon = 0, y = 0, c = 1, \lambda = 0.4, \kappa_1 = 0$ and $\kappa_2 = 0$.

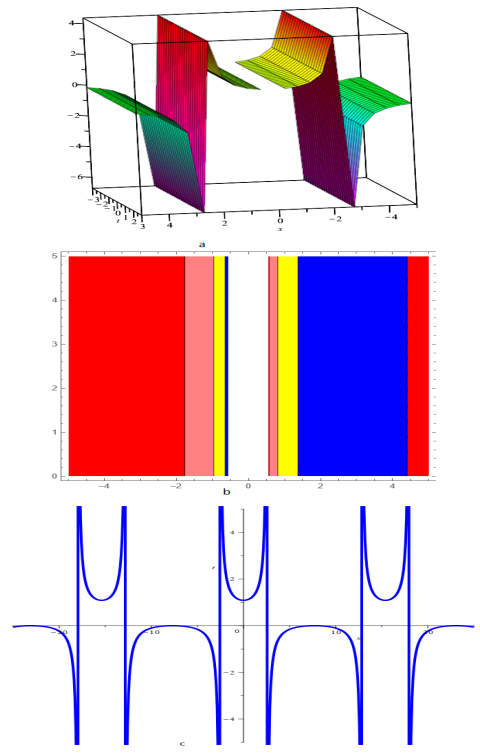


Figure 3 Figures (a),(b) and (c) represents 3D, Contour and 2D plots respectively $\Psi_4(x, y, t)$ corresponding to the values $\kappa = 0.5, \epsilon = 0, y = 0, c = 1, \lambda = 0.4, \kappa_1 = 0$ and $\kappa_2 = 0$

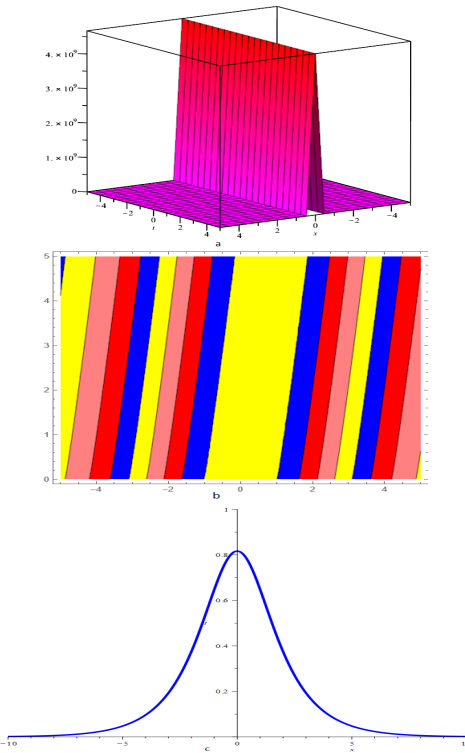


Figure 2 Figures (a),(b) and (c) represents 3D, Contour and 2D plots respectively $\Psi_9(x, y, t)$ corresponding to the values $\kappa = 0.5, \epsilon = 0, y = 0, c = 1, \lambda = 0.4, \kappa_1 = 0$ and $\kappa_2 = 0$.

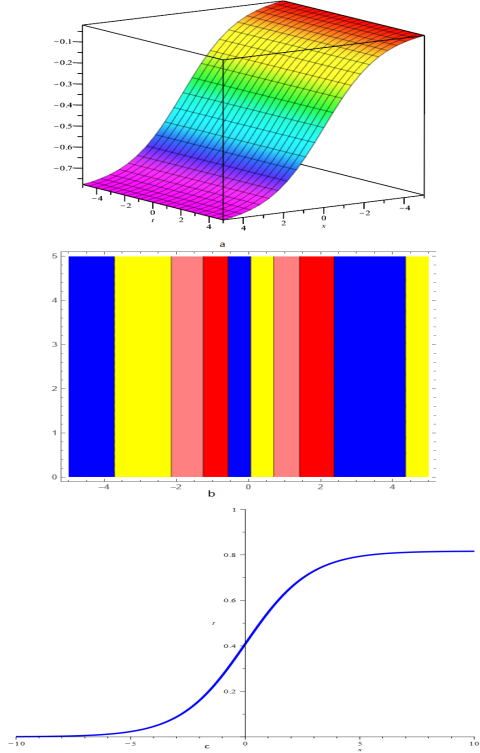


Figure 4 Figures (a),(b) and (c) represents 3D, Contour and 2D plots respectively $\Psi_5(x, y, t)$ corresponding to the values $\kappa = 0.5, \epsilon = 0, y = 0, c = 1, \lambda = 0.4, \kappa_1 = 0$ and $\kappa_2 = 0$

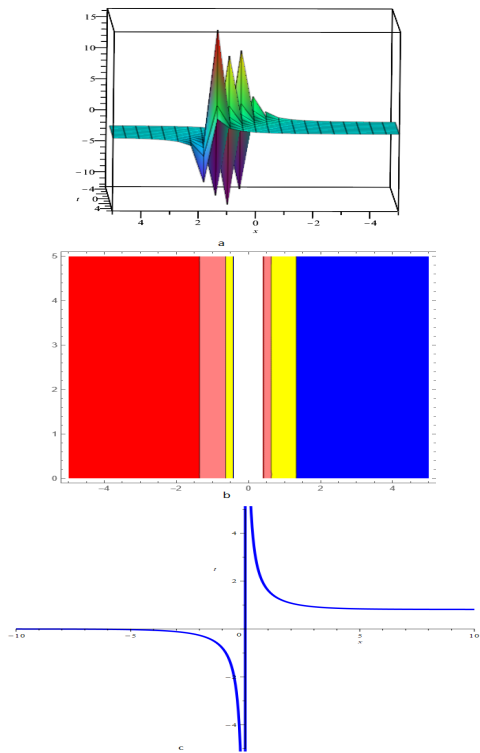


Figure 5 Figures (a),(b) and (c) represents 3D, Contour and 2D plots respectively $\Psi_6(x, y, t)$ corresponding to the values $\kappa = 0.5, \epsilon = 0, y = 0, c = 1, \lambda = 0.4, \kappa_1 = 0$ and $\kappa_2 = 0$

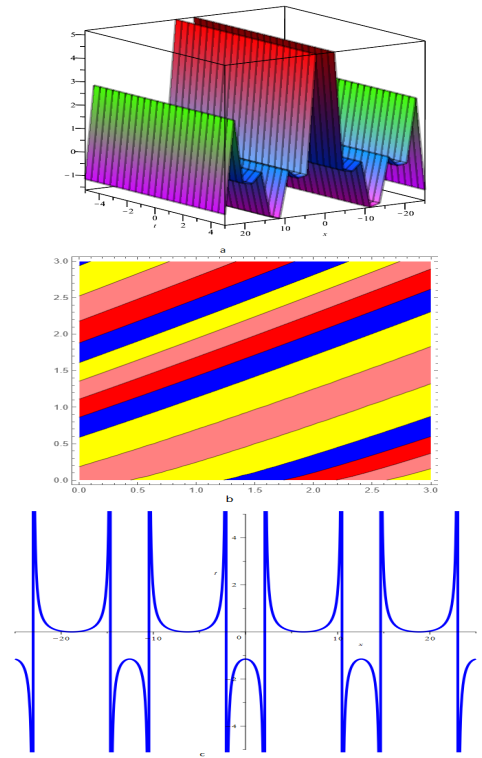


Figure 7 Figures (a),(b) and (c) represents 3D, Contour and 2D plots respectively $\Psi_4(x, y, t)$ corresponding to the values $\kappa = 0.5, \epsilon = 0, y = 0, c = 1, \lambda = 0.4, \kappa_1 = 0$ and $\kappa_2 = 0.5$

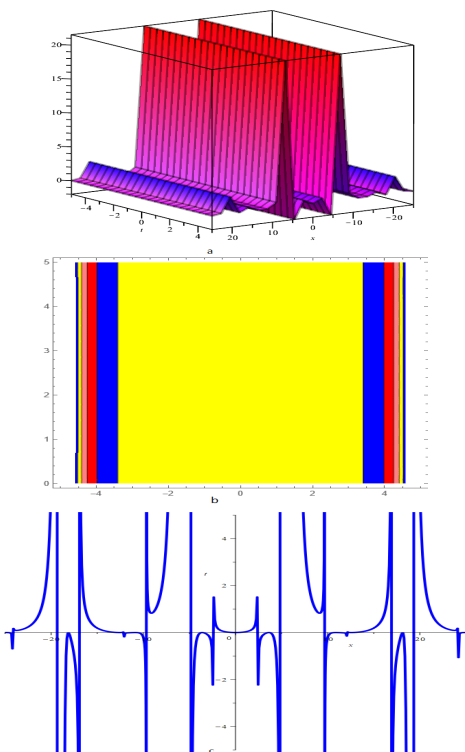


Figure 6 Figures (a),(b) and (c) represents 3D, Contour and 2D plots respectively $\Psi_3(x, y, t)$ corresponding to the values $\kappa = 0.5, \epsilon = 0, y = 0, c = 1, \lambda = 0.4, \kappa_1 = 0$ and $\kappa_2 = 0.5$

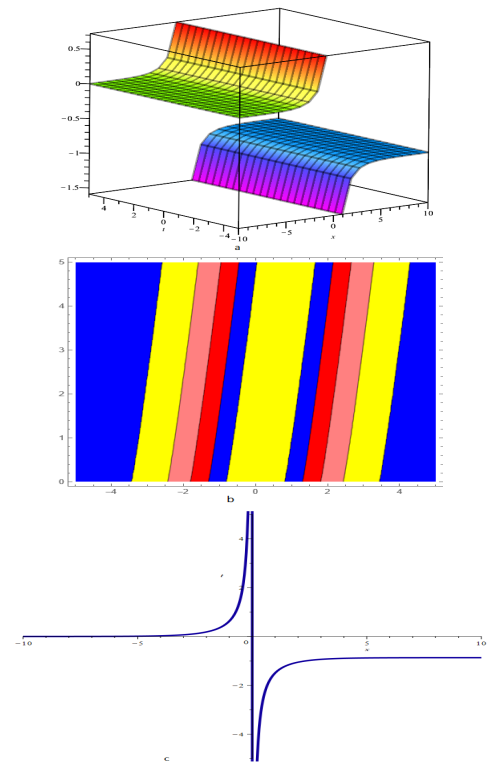


Figure 8 Figures (a),(b) and (c) represents 3D, Contour and 2D plots respectively $\Psi_6(x, y, t)$ corresponding to the values $\kappa = 0.5, \epsilon = 0, y = 0, c = 1, \lambda = 0.4, \kappa_1 = 0$ and $\kappa_2 = 0.5$

BIFURCATION ANALYSIS OF THE MODEL

For the sake of bifurcation analysis through phase portrait of Eq.(7), suppose that $\Psi' = \chi$ then Eq.(7) transform into the first order dynamical system of the following form:

$$\begin{cases} \frac{d\Psi}{d\zeta} = \chi, \\ \frac{d\chi}{d\zeta} = \eta_1\Psi - \eta_2\Psi^3, \end{cases} \quad (36)$$

where $\eta_1 = \frac{\theta + \kappa_1^2}{\lambda^2}$, and $\eta_2 = \frac{(1 + \kappa_2 + c)^2}{\lambda^2(2\kappa_1 - 1)}$. Hamiltonian function for the dynamical system (36) is defined as:

$$L(\Psi, \chi) = \frac{\chi^2}{2} - \eta_1 \frac{\Psi^2}{2} + \eta_2 \frac{\Psi^4}{4}. \quad (37)$$

The dynamical system (36) has the following equilibrium points:

$$Y_1 = (0, 0), \quad Y_2 = \left(\sqrt{\frac{\eta_1}{\eta_2}}, 0\right), \quad Y_3 = \left(-\sqrt{\frac{\eta_1}{\eta_2}}, 0\right).$$

Furthermore, the Jacobian of (36) is:

$$J(\Psi, \chi) = \begin{vmatrix} 0 & 1 \\ \eta_1 - 3\eta_2\Psi^2 & 0 \end{vmatrix}$$

$$= -\eta_1 + 3\eta_2\Psi^2,$$

thus (Ψ, χ) is a saddle point for $J(\Psi, \chi) < 0$, a center for $J(\Psi, \chi) > 0$ and a cusp if $J(\Psi, \chi) = 0$.

To investigate the characteristics of the system (36), we consider the different possible cases by taking various values of parameters and observe the corresponding critical points, the following cases are observed and analysed as:

• **Case 1:** Let $\eta_1 > 0$, and $\eta_2 > 0$.

For $\theta = 0.5$, $c = 1$, $\lambda = 0.4$, $\kappa_1 = 0$ and $\kappa_2 = 0$, system (36), then critical points $Y_1 = (0, 0)$, $Y_2 = (-0.57735, 0)$, and $Y_3 = (0.57735, 0)$. In this case, Y_1 is **saddle point** and Y_2, Y_3 are **central points**. The phase plots are displayed for different values of λ in Fig.(9).

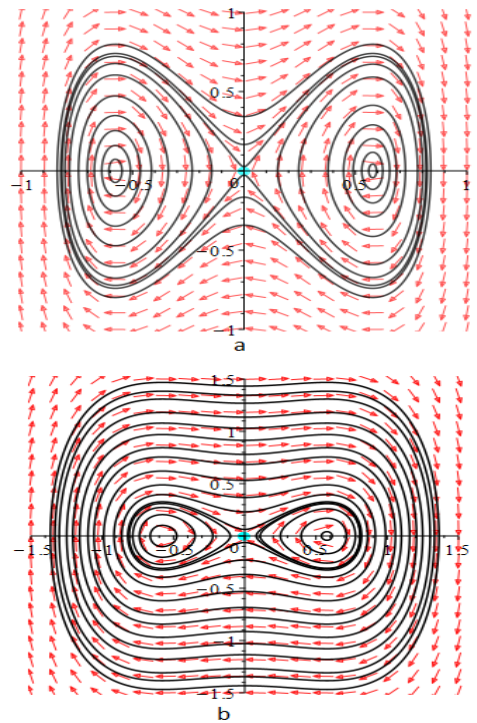


Figure 9 Phase Portarait visualization of the planar system (36) corresponding to the parameter values for Fig.(a) $\theta = 0.5$, $c = 1$, $\lambda = 0.4$, $\kappa_1 = 0$, $\kappa_2 = 0$ and Fig.(b) $\theta = 0.5$, $c = 1$, $\lambda = 0.9$, $\kappa_1 = 0$, $\kappa_2 = 0$

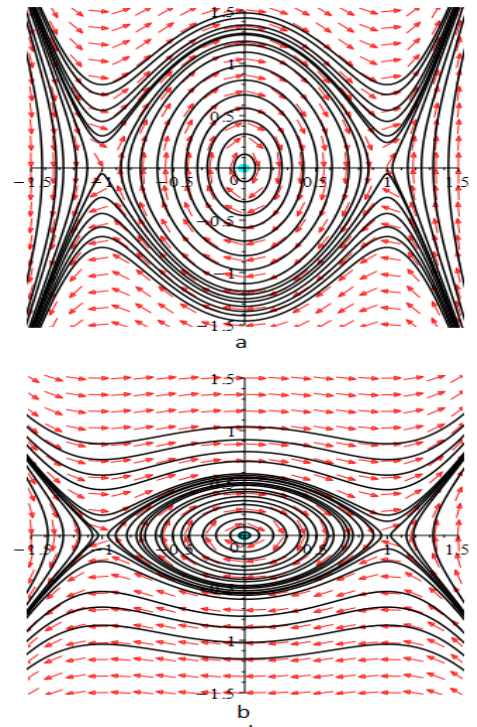


Figure 10 Phase Portarait visualization of the planar system (36) corresponding to the parameter values for Fig.(a) $\theta = -0.5$, $c = 1$, $\lambda = 0.4$, $\kappa_1 = 0$ and $\kappa_2 = 0$. and Fig.(b) $\theta = -0.5$, $c = 1$, $\lambda = 0.9$, $\kappa_1 = 0$, $\kappa_2 = 0$.

• **Case 2:** Let $\eta_1 < 0$, and $\eta_2 < 0$.

For $\theta = -0.5$, $c = 1$, $\lambda = 0.4$, $\kappa_1 = 0$ and $\kappa_2 = 0$, system (36) exhibits three fixed points $Y_1 = (0, 0)$, $Y_2 = (-1, 0)$, and $Y_3 = (1, 0)$. In this case, Y_1 is **center** and Y_2, Y_3 are **saddle points**. Also the phase plots are displayed for different values of λ in Fig.(10).

CONCLUSION

In this study, we effectively explored a novel mapping method to complex three coupled Maccari's system to unveil novel soliton solutions. This is achieved through the utilization of M-Truncated fractional derivative with employing the new mapping method and Maple software. Our study elucidates a variety of soliton solutions. These versatile soliton classifications provide flexible tools for both modeling and simulation purposes. To the best of our understanding, this technique has been employed for the first time on this model, resulting in entirely novel solutions not previously documented in the existing literature. To facilitate comprehension, with certain solutions being visually depicted through 2-dimensional, contour, 3-dimensional plots and phase portraits depicting bifurcation characteristics that explored comprehensively its dynamical nature at equilibrium points utilizing Maple software. Fundamentally, grasping the dynamic characteristics of systems holds significant value in predicting results and propelling advancements in emerging technologies. In summary, the results of this investigation are not only intriguing but also highlight the effectiveness of the suggested methodologies in evaluating the dynamics of solitons and phase patterns across various nonlinear models.

Author's Contribution

Writing original draft, M.B.R. and A.R; Writing review and editing, Methodology, Conceptualization, formal analysis A.R. and M.B.R.; Software, Supervision, Funding, M.B.R.; Project administration, Visualization, Formal analysis A.J.

Acknowledgments

This article has been produced with the financial support of the European Union under the REFRESH – Research Excellence For Region Sustainability and High-tech Industries project number CZ.10.03.01/00/22_003/0000048 via the Operational Programme Just Transition.

Availability of data and material

Not applicable.

Conflicts of interest

The authors declare that there is no conflict of interest regarding the publication of this paper.

Ethical standard

The authors have no relevant financial or non-financial interests to disclose.

LITERATURE CITED

- A. Filiz, M. E. and A. Sonmezoglu, 2014 F-expansion method and new exact- solution of the Schrödinger-KdV equation . Sci. World J. **2014**.
- Alabedalhadi, A.-O. S.-A.-S.-M., M. and S. Alhazmi, 2023 Traveling Wave Solutions for Time-Fractional mKdV-ZK Equation of Weakly Nonlinear Ion-Acoustic Waves in Magnetized Electron-Positron Plasma . Symmetry **15**.
- Das, N. and S. Saha Ray, 2022 Dispersive optical soliton wave solutions for the time-fractional perturbed nonlinear Schrödinger equation with truncated M-fractional conformable derivative in the nonlinear optical fibers. Opt. Quantum Electron **54**.
- Das, N. and S. Saha Ray, 2023 Dispersive optical soliton solutions of the (2+1)-dimensional cascaded system governing by coupled nonlinear Schrödinger equation with Kerr law nonlinearity in plasma. Opt. Quantum Electron **55**.
- E. M. Zayed, R. M. S. A. B. Y. Y. A. S. A., M. E. Alngar and H. M. Alshehr, 2022 Optical solitons having Kudryashov's self-phase modulation with multiplicative white noise via Itô Calculus using new mapping approach. Optik **264**.
- Ellahi, M.-D. S., R. and U. Khan, 2018 Exact traveling wave solutions of fractional order Boussinesq-like equations by applying Exp-function method. Results in Phys **8**: 114–120.
- Emad, Z.-M. S. S. M.-A. M., H.M. and A. Lanre, 2021 Exact propagation of the isolated waves model described by the three coupled nonlinear Maccari's system with complex structure. . Int. J. Mod. Phys. B **35**.
- Ge, Z.-M. and C.-Y. Ou, 2008 Chaos synchronization of fractional order modified Duffing systems with parameters excited by a chaotic signal. Chaos Solitons Fractals **35**: 705–717.
- Khater, B. N. K., M.M.A. Ghanbari and D. Kumar, 2020 Novel exact solutions of the fractional Bogoyavlensky–Konopelchenko equation involving the Atangana-Baleanu-Riemann derivative. Alex. Eng. J. **59**: 2957–2967.
- Mohammed, E.-M. M. M. A.-A. E. B. M., W.W. and A. Abouelregal, 2023 Effects of M-Truncated Derivative and Multiplicative Noise on the Exact Solutions of the Breaking Soliton Equation. . Symmetry **15**.
- Naeem, R.-H. K. A. S.-R., M. and S. Zaland, 2022 Analysis of the fuzzy fractional-order solitary wave solutions for the KdV equation in the sense of Caputo-Fabrizio derivative. . J. Math. **2022**: 2957–2967.
- Rafiq, M.-A. I. M., M.N. and M. Kamran, 2022 New traveling wave solutions for space-time fractional modified equal width equation with beta derivative. Phys. Lett. A **446**: 411–425.
- Saha Ray, S. and N. Das, 2022 Novel optical soliton solutions for time-fractional resonant nonlinear Schrödinger equation in optical fiber. . Mod.Phys. Lett. B **36**.
- Senol, M., 2020 New analytical solutions of fractional symmetric regularized-long-wave equation. Rev. Mex. Fís. **66**: 297–307.
- Vanterler, D. C. E. O.-D., J.; Sousa, 2018 A new truncated M-fractional derivative type unifying some fractional derivative types with classical properties. Int. J. Anal. Appl **16**: 83–96.
- W. B. Rabie, H. M. A. and W. Hamdy, 2023 Exploration of new optical solitons in magneto-optical waveguide with coupled system of nonlinear Biswas–Milovic equation via Kudryashov's law using extended F-expansion method. . Mathematics **11**.
- Wang, S. C.-Q. L.-X.-Q., Y.-Y. and J.-G. Li, 2018 Nonautonomous solitons for an extended forced Korteweg-de Vries equation with variable coefficients in the fluid or plasma. Waves Random Complex Media **3**: 411–425.
- X. Zeng, X. Y., 2008 A new mapping method and its applications

- to nonlinear partial differential equations. Phys. Lett. A **372**: 6602–6607.
- Zaslavsky, G., 2002 Chaos, fractional kinetics, and anomalous transport. Phys. Rep. **371**: 461–580.
- Zayed, E. M. and K. A. AlurrÖ, 2017 Solitons and other solutions for two nonlinear Schrödinger equations using the new mapping method. Optik **11**: 132–148.
- Zayed, E. M. E. and K. A. E. AlurrÖ, 2015 A new Jacobi elliptic function expansion method for solving a nonlinear PDE describing the nonlinear low-pass electrical lines, Chaos, Solitons and Fractals. . Mathematics **78**: 148–155.
- Zheng, B. and Q. Feng, 2014 The Jacobi elliptic equation method for solving fractional partial differential equations . Abs. Appl. Anal. **2014**.
- Zhu, L. Z. X.-Y., W. and M. Gao, 2023 Bifurcations and the Exact Solutions of the Time-Space Fractional Complex Ginzburg-Landau Equation with Parabolic Law Nonlinearity. Fractal Fract. **7**.

How to cite this article: Riaz, M. B., Rehman, A. U., and Martinovic, J. Application of the New Mapping Method to Complex Three Coupled Maccari's System Possessing M-Fractional Derivative. *Chaos Theory and Applications*, 6(3), 180-191, 2024.

Licensing Policy: The published articles in CHTA are licensed under a [Creative Commons Attribution-NonCommercial 4.0 International License](https://creativecommons.org/licenses/by-nc/4.0/).

